

Downregulation of Annexin A1 is correlated with radioresistance in nasopharyngeal carcinoma

LIFANG HUANG^{1*}, LI LIAO^{1*}, YANPING WAN¹, AILAN CHENG²,
MEIXIANG LI², SIHAN CHEN¹, MAOYU LI³, XING TAN¹ and GUQING ZENG¹

¹Institute of Nursing Research, School of Nursing; ²Cancer Research Institute, School of Medicine, University of South China, Hengyang, Hunan 421001; ³Key Laboratory of Cancer Proteomics of Chinese Ministry of Health, Xiangya Hospital, Central South University, Changsha, Hunan 410008, P.R. China

Received May 26, 2015; Accepted September 30, 2016

DOI: 10.3892/ol.2016.5324

Abstract. Radiotherapy is the primary treatment for nasopharyngeal carcinoma (NPC), but radioresistance often remains an obstacle to successful treatment. In our previous study, it was demonstrated that Annexin A1 (ANXA1) was involved in the p53-mediated radioresponse in NPC cells, which suggested that it may be associated with radioresistance in NPC; however, the role of ANXA1 in NPC radioresistance is unknown. In the present study, CNE2 cells were stably transfected with pLKO.1-ANXA1-small hairpin (sh)RNAs to investigate the effects of ANXA1 on the radiosensitivity of NPC. CNE2 cells transfected with pLKO.1 were used as the control. The radiosensitivities of the cells *in vitro* were analyzed using the clonogenic survival assay, cell growth analysis, flow cytometry and Hoechst 33258 staining. ANXA1 downregulation significantly enhanced clonogenic survival and cell growth following treatment of CNE2 cells with ionizing radiation (IR), increased the number of cells in the S phase and decreased IR-induced apoptosis. These results suggested that the radiosensitivity of CNE2 cells transfected with ANXA1-specific shRNA was significantly lower compared with the control cells. Therefore, ANXA1 downregulation may be involved in the radioresistance of NPC, and ANXA1 may be considered a novel biomarker for predicting NPC response to radiotherapy.

Introduction

Nasopharyngeal carcinoma (NPC) is an endemic disease in Southern China and Southeast Asia, where it has an incidence of 15-50 per 100,000 individuals. Therefore, NPC poses one of the most severe public health problems in these areas (1). The disease tends to be more sensitive to ionizing radiation (IR) than other head and neck cancers and, therefore, the primary treatment for patients with NPC is radiotherapy (2,3). Although the technology for radiotherapy has been improved, its therapeutic effects on NPC are unchanged. The main reason for this is the existence of radioresistant cells in NPC tissues. These cells not only show resistance to radiation, but they also exhibit an increased invasive ability following radiotherapy (2,4,5). Some patients with NPC present with local recurrence and distant metastases following radiotherapy due to radioresistance. The majority of these patients succumb to recurrence and metastasis within 1.5 years of treatment (6,7). Therefore, radioresistance leading to local recurrence has emerged as a major obstacle to the successful treatment of NPC. However, the molecular mechanisms underlying radioresistance in NPC remain unclear, and reliable molecular markers for predicting the radiosensitivity of NPC are limited.

The annexins are a well-known, closely related, multigene superfamily of Ca²⁺-regulated, phospholipid-dependent and membrane-binding proteins (8,9). As a member of the annexins, Annexin A1 (ANXA1) participates in numerous biological processes, including cellular transduction, membrane aggregation, inflammation, proliferation, differentiation and apoptosis. Accumulating evidence has suggested that ANXA1 dysregulation is associated with the occurrence, development, invasion, metastasis and drug resistance of hepatocellular carcinoma, endometrial carcinoma, melanoma, prostate cancer and esophageal cancer (9); however, the role of ANXA1 in NPC radioresistance remains unknown.

In our previous study, it was demonstrated that p53 was involved in the cellular response to IR in NPC cells, and ANXA1 was involved in the p53-mediated radioresponse in NPC cells; thus suggesting that ANXA1 may be associated with the radioresistance of NPC (10). To investigate the role of ANXA1 in the radioresistance of NPC, the present study knocked-down ANXA1 expression in the human CNE2 NPC

Correspondence to: Professor Guqing Zeng, Institute of Nursing Research, School of Nursing, University of South China, 28 Changsheng Road West, Hengyang, Hunan 421001, P.R. China
E-mail: zengguqing0123@163.com

*Contributed equally

Abbreviations: NPC, nasopharyngeal carcinoma; siRNA, small interfering RNA; IR, ionizing radiation; ANXA1, Annexin A1

Key words: Annexin A1, nasopharyngeal carcinoma, ionizing radiation, radioresistance

cell line using small hairpin (sh)RNAs targeting ANXA1, and then analyzed the radiosensitivity of the cells to IR *in vitro*. The results suggested that ANXA1 was associated with the radioresistance of NPC, and that ANXA1 downregulation may increase the radioresistance of NPC. These findings indicated that ANXA1 may be as a potential biomarker for predicting NPC response to radiotherapy and it may be beneficial for the development of personalized therapeutic strategies.

Materials and methods

Cell lines and culture. The human CNE2 NPC cell line was obtained from the Key Laboratory of Cancer Proteomics of the Chinese Ministry of Health of Xiangya Hospital (Changsha, China). The cells were cultured in Dulbecco's modified Eagle's medium (DMEM; Invitrogen; Thermo Fisher Scientific, Inc., Waltham, MA, USA) supplemented with 10% fetal bovine serum (Invitrogen; Thermo Fisher Scientific, Inc.). Cells were maintained at 37°C in a humidified 5% CO₂ atmosphere.

Transfection of CNE2 cells with ANXA1-specific shRNA plasmid. The ANXA1-specific shRNA plasmid, pLKO.1-ANXA1-shRNAs, and empty vector, pLKO.1, were purchased from GE Healthcare Life Sciences (Shanghai, China). For stable transfection, 1x10⁷ CNE2 cells were transfected with pLKO.1-ANXA1-shRNA or pLKO.1 using Lipofectamine 2000 reagent (Invitrogen; Thermo Fisher Scientific, Inc.), according to the manufacturer's protocol. After 14 days of selection in DMEM medium containing 1.0 µg/ml puromycin (Invitrogen; Thermo Fisher Scientific, Inc.), individual puromycin-resistant colonies were isolated and expanded. The expression of ANXA1 in these clones was confirmed by western blotting. CNE2 cells were termed CNE2-shANXA1 or CNE2-pLKO.1 following transfection with pLKO.1-ANXA1-shRNAs and the pLKO.1 empty vector, respectively.

Western blotting. The CNE2-shANXA1 and CNE2-pLKO.1 cells were dissolved in lysis buffer (150 mM NaCl, 50 mM Tris-Cl, pH 8.0; 0.1% NP-40, 1 mM phenylmethylsulfonyl fluoride and 25 µg/ml aprotinin and 25 µg/ml leupeptin), vortexed and incubated at room temperature for 2 h. The concentration of the total proteins in the supernatants was assayed using the Bradford assay (Bio-Rad Laboratories, Inc., Hercules, CA, USA). The expression levels of ANXA1 in the two NPC cell lines (CNE2-shANXA1 and CNE2-pLKO.1) were determined using western blotting, as described previously (11). Briefly, 30 µg lysates were separated by 8% SDS-PAGE and transferred onto polyvinylidene difluoride membranes (EMD Millipore, Billerica, MA, USA). The membranes were blocked with 5% nonfat dry milk for 2 h at room temperature, after which they were incubated with anti-ANXA1 (1:500; A3359; Sigma-Aldrich; Merck Millipore, Darmstadt, Germany) and anti-β-actin (1:3,000; A5228; Sigma-Aldrich; Merck Millipore) primary antibodies overnight at 4°C, followed by incubation with a horseradish peroxidase-conjugated secondary antibody (1:3,000; NXA931; GE Healthcare Life Sciences) for 1 h at room temperature. The signal was visualized using an

enhanced chemiluminescence detection reagent (Thermo Fisher Scientific, Inc.) and quantified by densitometry using the ImageQuant TL image analysis system (GE Healthcare Life Sciences).

Clonogenic survival assay. The radioresistance levels of the CNE2-shANXA1 and CNE2-pLKO.1 cells were measured using clonogenic survival assays following irradiation, as described previously (2). Briefly, the cells were plated into six-well culture plates (2x10³ cells/well) and exposed to a range of radiation doses (0-8 Gy). Following irradiation, the cells were cultured for 12 days and the survival colonies (defined as a colony with >50 cells) and their constituent cells were counted. The survival fraction (SF) was calculated as the number of colonies divided by the number of cells seeded multiplied by the plating efficiency. The plating efficiency was calculated as the number of colonies for every 10 cells. Dose modifying factors (DMFs) were calculated using the following equation: DMF = (dose to reach the specified survival in resistant cells) / (dose to reach the same survival in the control). The cells were plated in triplicate.

Cell viability analysis in response to irradiation. The cells were plated into 96-well culture plates (2x10³ cells/well). Following incubation for 12 h, the cells were exposed to 5-Gy irradiation. The cell viability was monitored using MTT assays after 1, 2, 3, 4, 5, 6 and 7 days following 5-Gy irradiation. Briefly, 20 µl of 5 mg/ml MTT (Sigma-Aldrich; Merck-Millipore) was added to each well every 24 h for 4 h. To dissolve the formazan crystals, 150 µl DMSO (Sigma-Aldrich; Merck Millipore) was added to each well for 10 min at room temperature. The absorbance of each well was read using the EL310 Microplate Autoreader (BioTek Instruments, Inc., Winooski, VT, USA) at 490 nm (A490). The percentage of viable cells was calculated by comparing with the A490 readings on the first day. All experiments were performed in triplicate.

Flow cytometry analysis of cell cycle distribution and apoptosis in response to irradiation. The cells were plated into T-50 flasks (2x10⁵ cells/flask), cultured for 12 h and then exposed to 5-Gy irradiation. Following culturing for 24 h, the cells were harvested, fixed with 70% ethanol (ice-cold) at -20°C for 1 h and then centrifuged at 1,225 x g for 5 min at 4°C. The pellets were incubated with 0.5% Triton X-100 (Sigma-Aldrich; Merck Millipore) and 0.05% RNase (Sigma-Aldrich; Merck Millipore) in 1 ml PBS at 37°C for 30 min, followed by centrifugation at 1,915 x g for 5 min at 4°C. Subsequently, the cell pellets were incubated with 40 µg/ml propidium iodide (Sigma-Aldrich; Merck Millipore) in 1 ml PBS at room temperature for 30 min. The cell cycle distribution and apoptosis were immediately detected by flow cytometry (BD Biosciences, San Jose, CA, USA). Three independent experiments were done.

Hoechst 33258 staining of apoptotic cells following irradiation. The cells were plated into 6-well culture plates (5x10³ cells/well), cultured for 12 h and then exposed to 5-Gy irradiation. Following culturing for 72 h, the cells were washed with PBS, fixed with 4% paraformaldehyde for 30 min at 4°C and stained with 5 µg/ml Hoechst 33258 (Sigma-Aldrich; Merck Millipore) dissolved in Hanks' buffer

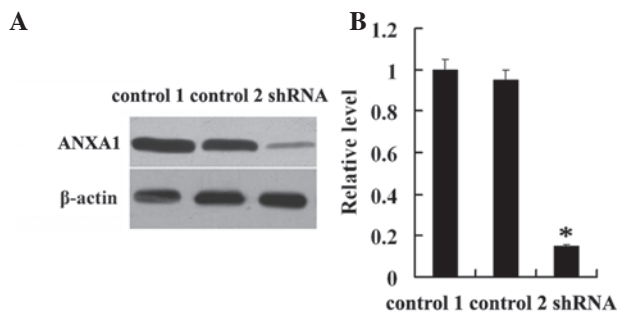


Figure 1. Establishment of the CNE2-shANXA1 cell line with knockdown of ANXA1. (A) Western blotting was used to detect the expression levels of ANXA1 in the untransfected (control 1), empty vector pLKO.1-transfected (control 2) and pLKO.1-ANXA1-shRNA-transfected CNE2 cells. (B) Histogram shows the expression levels of ANXA1 in the three cell lines as determined by densitometric analysis. β -actin was used as an internal loading control. * $P < 0.05$; CNE2-shANXA1 vs. control 1 or control 2. ANXA1, Annexin A1; shRNA, small hairpin RNA.

in the dark for 10 min. Apoptotic cells were identified on the basis of the presence of highly condensed or fragmented nuclei. To calculate the percentage of apoptotic cells, at least 200 cells from three different microscopic fields were counted.

Statistical analysis. Statistical analyses were performed using SPSS 17.0 software (SPSS Inc., Chicago, IL, USA). Data are presented as the mean \pm standard deviation. Significant differences between groups were determined using the Student's *t*-test. $P < 0.05$ was considered to be statistically significant.

Results

Establishment of the CNE2-shANXA1 cell line with knock-down of ANXA1. To determine whether downregulation of ANXA1 is involved in NPC radioresistance, CNE2 cells were transfected with the ANXA1-specific shRNA plasmid, pLKO.1-ANXA1-shRNAs or pLKO.1 empty vector and western blotting was used to detect the expression levels of ANXA1 in the NPC cell lines. As shown in Fig. 1, the expression level of ANXA1 in CNE2-shANXA1 cells was significantly lower compared with that in CNE2-pLKO.1 cells ($P < 0.01$). Conversely, there was no obvious difference in the expression levels of ANXA1 between CNE2 and CNE2-pLKO.1 cells ($P > 0.05$; Fig. 1). These results suggested that ANXA1 was successfully knocked-down in the CNE2-shANXA1 cells.

Effects of the downregulation of ANXA1 on the proliferation of NPC cells following irradiation in vitro. To detect the association between the expression level of ANXA1 and the radioresistance of NPC cells, CNE2-shANXA1 and CNE2-pLKO.1 cells were irradiated with a range of radiation doses (0-8 Gy) and examined using clonogenic survival assays. As shown in Fig. 2A, CNE2-shANXA1 cells formed more and larger survival colonies than CNE2-pLKO.1 cells. As shown in Fig. 2B, the radiosensitivity of CNE2-shANXA1 cells was decreased compared with that of CNE2-pLKO.1 cells. The DMFs were 1.85 and 1.57, respectively, at 10% and 1% isosurvival levels of CNE2-shANXA1 cells. The survival fraction at 2 Gy (SF2) was 0.51 for CNE2-pLKO.1 cells and

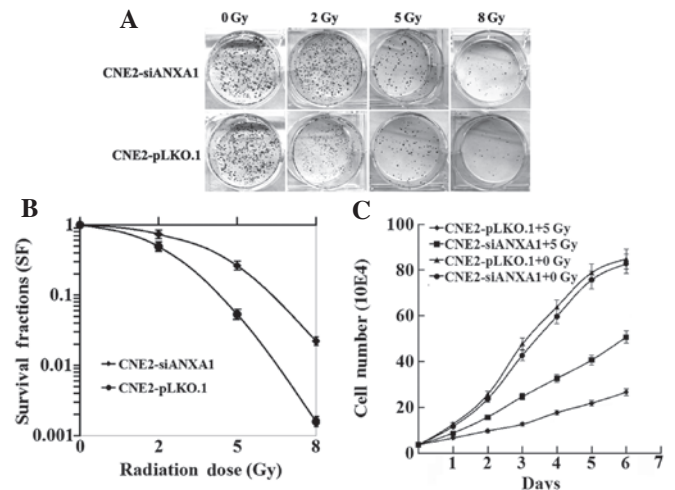


Figure 2. Different sensitivity to radiation in CNE2-shANXA1 and CNE2-pLKO.1 cells. (A and B) Clonogenic survival assay. CNE2-shANXA1 and CNE2-pLKO.1 cells plated onto six-well culture plates were irradiated with a range of radiation doses (0-8 Gy), and the number of colonies formed following incubation for 12 days were counted to calculate the survival fractions. (C) Viability assay. CNE2-shANXA1 and CNE2-pLKO.1 cells were seeded into 96-well culture plates 12 h prior to irradiation. The cell viability was monitored by performing MTT assays at different time intervals following 5-Gy irradiation. The viability of CNE2-shANXA1 and CNE2-pLKO.1 cells without 5-Gy irradiation, which were used as controls, is also shown. * $P < 0.05$; CNE2-shANXA1 vs. CNE2-pLKO.1. ANXA1, Annexin A1.

0.69 for CNE2-shANXA1 cells. Furthermore, the effect of ANXA1-knockdown on the viability of NPC cells following exposure to 5-Gy IR was examined. As shown in Fig. 2C, the rate at which the viability of the cells was decreased following 5-Gy irradiation was slower for CNE2-shANXA1 cells compared with CNE2-pLKO.1 cells. The results demonstrated that the radiosensitivity of CNE2-shANXA1 cells was significantly lower than that of CNE2-pLKO.1 cells.

Effects of ANXA1 downregulation on the apoptosis of NPC cells following irradiation. The apoptotic difference in response to radiation between CNE2-shANXA1 and CNE2-pLKO.1 cells was further assessed using flow cytometry and Hoechst 33258 staining. As shown in Fig. 3, Hoechst 33258 staining and flow cytometric analysis demonstrated that the rate of apoptosis of CNE2-shANXA1 cells was reduced compared with that of CNE2-pLKO.1 cells following irradiation. These results support the notion that ANXA1 downregulation is involved in the radioresistance of NPC.

Effects of ANXA1 downregulation on the cell cycle distributions of NPC cells following irradiation. The cell cycle progression and arrest in response to irradiation may determine the sensitivity of cells to irradiation. The cell cycle distributions of CNE2-shANXA1 and CNE2-pLKO.1 cells were analyzed at 24 h following exposure to 5-Gy irradiation using flow cytometry. As shown in Table I, there was no difference in the percentage of cells in the G0-G1 phases between the CNE2-shANXA1 and CNE2-pLKO.1 cells at 24 h following irradiation, whereas more CNE2-shANXA1 cells were observed in the S phase and less in the G2-M phase, as compared with the CNE2-pLKO.1 cells. These results suggest

Table I. Cell cycle distribution of CNE2-siANXA1 and CNE2-pLKO.1 cells at 24 h following 5-Gy irradiation.

Cell lines	Percentage of cells					
	G0/G1	P-value	S phase	P-value	G2/M	P-value
CNE2-siANXA1	58.2±3.1	0.3874	35.8±2.7	0.0016 ^a	6.0±0.8	<0.0001 ^a
CNE2-pLKO.1	62.7±3.6		24.5±2.4		12.8±1.3	

^aP<0.01 CNE2-siANXA1 vs. control CNE2-pLKO.1 cells by χ^2 test. ANXA1, Annexin A1.

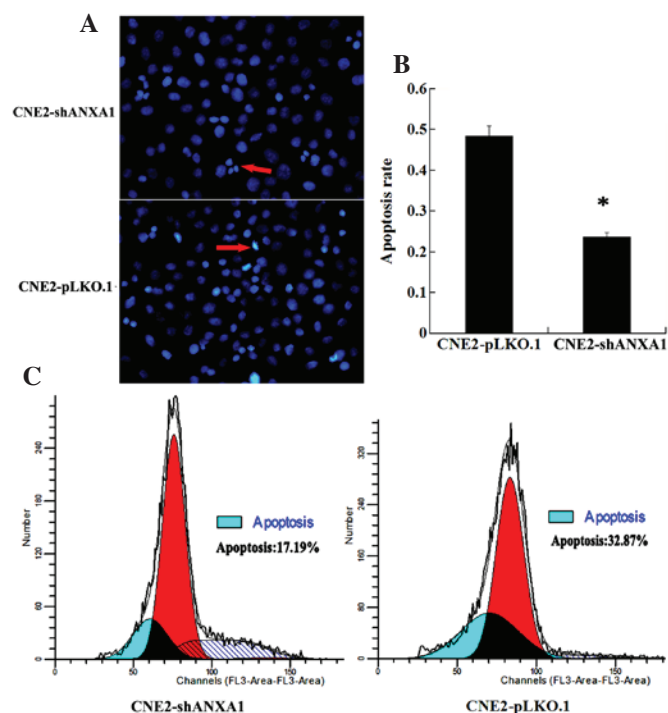


Figure 3. Different apoptotic rate of CNE2-shANXA1 and CNE2-pLKO.1 cells with radiation. (A) Hoechst 33258 staining of apoptotic cells. CNE2-shANXA1 and CNE2-pLKO.1 cells were exposed to 5-Gy irradiation, incubated for 72 h and then apoptosis was assessed using the cell-permeable DNA dye Hoechst 33258. The arrows indicate apoptotic nuclei with intense fluorescence corresponding to chromatin condensation. (B) A histogram showing the apoptotic rate of the two cell lines. Every sample was repeated three times. Data are presented as the mean \pm standard deviation. (C) Flow cytometry analysis of apoptotic cells. CNE2-shANXA1 and CNE2-pLKO.1 cells were exposed to 5-Gy irradiation, incubated for 24 h and then assessed for apoptosis by flow cytometry. ANXA1, Annexin A1. *P<0.05; CNE2 shANXA1 vs. CNE2 pLKO.1.

that changes to the cell cycle induced by IR may be altered in the radioresistant CNE2-shANXA1 cells, and that downregulation of ANXA1 may be closely related to the radioresistance of NPC.

Discussion

NPC is one of the most common malignant tumors in Southern China and Southeast Asia. NPC tends to be more sensitive to radiation than some other types of cancer and, therefore, radiotherapy is the primary treatment for patients with NPC (2). Nevertheless, the 5-year survival rate of patients with advanced NPC following radiotherapy is not satisfactory. It is reported

that the 5-year survival rate of stage I and II NPC ranges from 72-90% (12). Conversely, the 5-year survival rate falls to 55% for stage III NPC and 30% for stage IV NPC, which is due to the incidence of local recurrence being relatively high in advanced NPC (5,13). IR primarily leads to double-stranded DNA breaks, and DNA damage induced by IR is able to kill tumor cells via the cell death pathway (14). Radioresistance is a serious obstacle in the treatment of NPC (6,7). The molecular mechanisms underlying the response of NPC to IR are yet to be elucidated.

p53 is a pivotal tumor suppressor that induces apoptosis, cell cycle arrest and senescence in response to various stresses, and it also has an important role in the regulation of radiosensitivity (15). Swa *et al* (16) observed the downregulation of p53 in ANXA1^{-/-} cells at the transcriptional level, which suggested that ANXA1 may regulate p53 transcription. In our previous study, it was demonstrated that p53 was involved in the cellular response to IR in NPC cells, and that ANXA1 was involved in the p53-mediated radiation response in NPC cells (10). However, the role of ANXA1 in the radioresistance of NPC is poorly understood.

ANXA1, which was the first characterized member of the annexin superfamily, has been shown to bind to the cellular membrane in a calcium-dependent manner. Besides mediating inflammation, ANXA1 has also been reported to be involved in important physiopathological processes, including cell proliferation, differentiation, transduction, phagocytosis and apoptosis (16). In recent years, the role of ANXA1 in the malignant tumor has emerged as a research focus in oncology. Accumulating evidence has indicated that ANXA1 dysregulation is associated with the occurrence, development, invasion, metastasis and drug resistance of cancers (17-20). The research evidence indicated that ANXA1 may specifically function as either a tumor suppressor or an oncogene candidate for certain cancers depending on the particular type of tumor cells/tissues (9). The upregulation of ANXA1 has been correlated with the development of hepatocellular carcinoma, colorectal cancer, lung cancer, pancreatic cancer, melanoma, skin cancer and endometrial carcinoma (21-27). Furthermore, its downregulation, as well as the translocation of ANXA1, has been shown to be a positive indicator for the development, progression and metastasis of prostate cancer, esophageal cancer, oral carcinoma, cervical cancer, intestinal-type sinonasal adenocarcinoma and NPC (17-19,28,29). Yu *et al* (20) reported that the expression of ANXA1 was downregulated in the adriamycin-resistant cell line (pumc-91/ADM) compared with its parental cell line (pumc-91). Zhu *et al* (30) detected the downregulation of ANXA1 in an adriamycin-resistant human

erythroleukemia cell line (K562/ADR) by matrix-assisted laser desorption/ionization time-of-flight tandem mass spectrometry and western blotting. They also demonstrated that the suppression of ANXA1 expression was able to reduce adriamycin chemosensitivity in K562/ADR cells (30). Although ANXA1 has important roles in chemoresistance, the role of ANXA1 in the radioresistance of NPC is still unknown.

In the present study, to determine the effect of ANXA1 on NPC cellular radiosensitivity, the NPC CNE2-shANXA1 cell line with stable knockdown of ANXA1 and the CNE2-pLKO.1 control cell line were established. These provided a unique pair of cell lines for studying the function of ANXA1 in NPC radioresistance, including changes in the biological characteristics of CNE2 cells following irradiation. The present study demonstrated that CNE2-shANXA1 cells formed more and larger survival colonies compared with CNE2-pLKO.1 cells using clonogenic survival assays. Furthermore, MTT assays demonstrated that the reduction in cell viability following irradiation was slower for CNE2-shANXA1 cells compared with control CNE2-pLKO.1 cells. Hoechst 33258 staining and flow cytometric analysis of apoptotic cells demonstrated that the rate of radiation-induced apoptosis was decreased in CNE2-shANXA1 cells compared with CNE2-pLKO.1 cells. In addition, flow cytometric analysis of the cell cycle distributions of CNE2-shANXA1 and CNE2-pLKO.1 cells at 24 h following exposure to 5-Gy irradiation suggested that there was no difference in the percentage of cells in the G0-G1 phases, whereas more CNE2-shANXA1 cells were observed to be detained in the S phase and less cells were observed in the G2-M phase, as compared with CNE2-pLKO.1 cells. Together, these findings indicated that ANXA1 may participate in cellular responses to IR in NPC cells.

It is well known that radioresistance is associated with DNA damage repair, apoptosis and cell cycle checkpoints (31-33). IR is able to induce DNA damage and apoptosis via reactive oxygen species generated by radiolytic hydrolysis (34). In a previous study, pathway analysis of stable isotope labeling with amino acids in cell culture data showed that ANXA1 has important roles in the DNA damage response and related pathways (16). Apoptosis has a crucial role in the cellular death pathway following exposure to IR, and previous studies have suggested that apoptosis is an important mechanism for radiotherapy (35,36). ANXA1 has been implicated in the apoptotic cell 'eat me' signal and ensuing phagocytosis. Yang *et al* (37) demonstrated that inhibition of protein kinase R-like endoplasmic reticulum kinase (PERK) or phosphoinositide 3-kinase (PI3K)/Akt diminished p22 and ANXA1 cell surface exposure, indicating that the PERK/PI3K/Akt signaling pathway mediates p22 and ANXA1 expression on the cell surface and further induces the 'eat-me' signal. It has been reported that ANXA1 is a proapoptotic protein that can regulate tumor necrosis factor-related apoptosis-inducing ligand-induced cell death in follicular thyroid carcinoma cells through the regulation of B-cell lymphoma-2/Bcl-XL-associated death promoter activity and translocation to the mitochondria (38). In the present study, apoptotic cells were detected using Hoechst 33258 staining and flow cytometry, and it was found that ANXA1 silencing was able to reduce radiation-induced apoptosis of CNE2 cells. These results suggested that the downregulation of ANXA1 enhances NPC radioresistance by inhibiting apoptosis.

The radiosensitivity of tumor cells is different during the different stages of the cell cycle. In general, cells are most sensitive to radiation-induced DNA damage during the G2 and M phases, and are most resistant to IR during the latter part of the S phase (39). Tell *et al* (40) reported that the proportion of S-phase cells was markedly increased for the lymphocytes from patients showing no response to radiotherapy, as compared with those from patients showing a partial or complete response. The results of the cell cycle distribution analysis in the present study showed that a high percentage of CNE2-shANXA1 cells were in the S phase following irradiation, while the CNE2-pLKO.1 cells were predominantly in the G2/M arrest. These findings indicated that stable inhibition of ANXA1 by shRNA was able to promote the arrest of CNE2 cells with DNA damage in the S phase, and decrease the radiosensitivity of CNE2 cells by impacting the cell cycle distribution.

In conclusion, the results of the present study suggested that ANXA1 may play an important role in the radioresistance of NPC, and inhibition of ANXA1 may increase the radioresistance of CNE2 cells by increasing colony growth, reducing apoptosis and altering cell cycle progression. Therefore, ANXA1 may be considered a novel biomarker for predicting the radiosensitivity of NPC. However, the accurate molecular mechanisms underlying the role of ANXA1 in NPC radioresistance remain unclear, and should be investigated in further studies.

Acknowledgements

This study was supported by the National Natural Science Foundation of China (grant nos. 81272959, 81470130, 81072198 and 81072199) and the Postgraduate Research Project of the University of South China (grant no. 2015XCX41).

References

1. Ho JH: An epidemiologic and clinical study of nasopharyngeal carcinoma. *Int J Radiat Oncol Biol Phys* 4: 182-198, 1978.
2. Feng XP, Yi H, Li MY, Li XH, Yi B, Zhang PF, Li C, Peng F, Tang CE, Li JL, *et al*: Identification of biomarkers for predicting nasopharyngeal carcinoma response to radiotherapy by proteomics. *Cancer Res* 70: 3450-3462, 2010.
3. Qu C, Liang Z, Huang J, Zhao R, Su C, Wang S, Wang X, Zhang R, Lee MH and Yang H: MiR-205 determines the radioresistance of human nasopharyngeal carcinoma by directly targeting PTEN. *Cell Cycle* 11: 785-796, 2012.
4. Teo P, Yu P, Lee WY, Leung SF, Kwan WH, Yu KH, Choi P and Johnson PJ: Significant prognosticators after primary radiotherapy in 903 nondisseminated nasopharyngeal carcinoma evaluated by computer tomography. *Int J Radiat Oncol Biol Phys* 36: 291-304, 1996.
5. DeNittis AS, Liu L, Rosenthal DI and Machtay M: Nasopharyngeal carcinoma treated with external radiotherapy, brachytherapy, and concurrent/adjunct chemotherapy. *Am J Clin Oncol* 25: 93-95, 2002.
6. Lee AW, Poon YF, Foo W, Law SC, Cheung FK, Chan DK, Tung SY, Thaw M and Ho JH: Retrospective analysis of 5037 patients with nasopharyngeal carcinoma treated during 1976-1985: Overall survival and patterns of failure. *Int J Radiat Oncol Biol Phys* 23: 261-270, 1992.
7. Leung SF, Teo PM, Shiu WW, Tsao SY and Leung TW: Clinical features and management of distant metastases of nasopharyngeal carcinoma. *J Otolaryngol* 20: 27-29, 1991.
8. Blackwood RA and Ernst JD: Characterization of Ca²⁺(+)-dependent phospholipid binding, vesicle aggregation and membrane fusion by annexins. *Biochem J* 266: 195-200, 1990.
9. Guo C, Liu S and Sun MZ: Potential role of Anxa1 in cancer. *Future Oncol* 9: 1773-1793, 2013.

10. Zeng GQ, Yi H, Li XH, Shi HY, Li C, Li MY, Zhang PF, Feng XP, Wan XX, Qu JQ, *et al*: Identification of the proteins related to p53-mediated radioresponse in nasopharyngeal carcinoma by proteomic analysis. *J Proteomics* 74: 2723-2733, 2011.
11. Zeng GQ, Zhang PF, Deng X, Yu FL, Li C, Xu Y, Yi H, Li MY, Hu R, Zuo JH, *et al*: Identification of novel biomarkers for early detection of human lung squamous cell cancer by quantitative proteomics. *Mol Cell Proteomics* 11: M111.013946, 2012.
12. Tulalamba W and Janvilisri T: Nasopharyngeal carcinoma signaling pathway: An update on molecular biomarkers. *Int J Cell Biol* 2012: 594681, 2012.
13. Chang JT, Ko JY and Hong RL: Recent advances in the treatment of nasopharyngeal carcinoma. *J Formos Med Assoc* 103: 496-510, 2004.
14. Vignard J, Mirey G and Salles B: Ionizing-radiation induced DNA double-strand breaks: A direct and indirect lighting up. *Radiother Oncol* 108: 362-369, 2013.
15. Zheng R, Yao Q, Du S, Ren C, Sun Q, Xu Z, Lin X and Yuan Y: The status of p53 in cancer cells affects the role of autophagy in tumor radiosensitisation. *J BUON* 19: 336-341, 2014.
16. Swa HL, Blackstock WP, Lim LH and Gunaratne J: Quantitative proteomics profiling of murine mammary gland cells unravels impact of annexin-1 on DNA damage response, cell adhesion and migration. *Mol Cell Proteomics* 11: 381-393, 2012.
17. Xia SH, Hu LP, Hu H, Ying WT, Xu X, Cai Y, Han YL, Chen BS, Wei F, Qian XH, *et al*: Three isoforms of annexin I are preferentially expressed in normal esophageal epithelia but down-regulated in esophageal squamous cell carcinomas. *Oncogene* 21: 6641-6648, 2002.
18. Zhang L, Yang X, Zhong LP, Zhou XJ, Pan HY, Wei KJ, Li J, Chen WT and Zhang ZY: Decreased expression of Annexin A1 correlates with pathologic differentiation grade in oral squamous cell carcinoma. *J Oral Pathol Med* 38: 362-370, 2009.
19. Cheng AL, Huang WG, Chen ZC, Peng F, Zhang PF, Li MY, Li F, Li JL, Li C, Hong Y, *et al*: Identification of novel nasopharyngeal carcinoma biomarkers by laser capture micro dissection and proteomic analysis. *Clin Cancer Res* 14: 435-445, 2008.
20. Yu S, Meng Q, Hu H and Zhang M: Correlation of ANXA1 expression with drug resistance and relapse in bladder cancer. *Int J Clin Exp Pathol* 7: 5538-5548, 2014.
21. Suo A, Zhang M, Yao Y, Zhang L, Huang C, Nan K and Zhang W: Proteome analysis of the effects of sorafenib on human hepatocellular carcinoma cell line HepG2. *Med Oncol* 29: 1827-1836, 2012.
22. He ZY, Wen H, Shi CB and Wang J: Up-regulation of hnRNP A1, Ezrin, tubulin b-2C and Annexin A1 in sentinel lymph nodes of colorectal cancer. *World J Gastroenterol* 16: 4670-4676, 2010.
23. Biaoxue R, Xiling J, Shuanying Y, Wei Z, Xiguang C, Jinsui W and Min Z: Upregulation of Hsp90-beta and annexin A1 correlates with poor survival and lymphatic metastasis in lung cancer patients. *J Exp Clin Cancer Res* 31: 70, 2012.
24. Bai XF, Ni XG, Zhao P, Liu SM, Wang HX, Guo B, Zhou LP, Liu F, Zhang JS, Wang K, *et al*: Overexpression of annexin 1 in pancreatic cancer and its clinical significance. *World J Gastroenterol* 10: 1466-1470, 2004.
25. Rondepierre F, Bouchon B, Papon J, Bonnet-Duquennoy M, Kintossou R, Moins N, Maublant J, Madelmont JC, D'Incan M and Degoul F: Proteomic studies of B16 lines: Involvement of annexin A1 in melanoma dissemination. *Biochim Biophys Acta* 1794: 61-69, 2009.
26. Hummerich L, Müller R, Hess J, Kokocinski F, Hahn M, Fürstenberger G, Mauch C, Lichter P and Angel P: Identification of novel tumour-associated genes differentially expressed in the process of squamous cell cancer development. *Oncogene* 25: 111-121, 2006.
27. Voisin SN, Krakovska O, Matta A, DeSouza LV, Romaschin AD, Colgan TJ and Siu KW: Identification of novel molecular targets for endometrial cancer using a drill-down LC-MS/MS approach with iTRAQ. *PLoS One* 6: e16352, 2011.
28. D'Acunto CW, Fontanella B, Rodriguez M, Taddei M, Parente L and Petrella A: Histone deacetylase inhibitor FR235222 sensitizes human prostate adenocarcinoma cells to apoptosis through upregulation of annexin A1. *Cancer Lett* 295: 85-91, 2010.
29. Rodrigo JP, García-Pedrero JM, Llorente JL, Fresno MF, Allonca E, Suarez C and Hermsen M: Down-regulation of annexin A1 and A2 protein expression in intestinal-type sinonasal adenocarcinomas. *Hum Pathol* 42: 88-94, 2011.
30. Zhu F, Wang Y, Zeng S, Fu X, Wang L and Cao J: Involvement of annexin A1 in multidrug resistance of K562/ADR cells identified by the proteomic study. *OMICS* 13: 467-476, 2009.
31. Tanaka T, Munshi A, Brooks C, Liu J, Hobbs ML and Meyn RE: Gefitinib radiosensitizes non-small cell lung cancer cells by suppressing cellular DNA repair capacity. *Clin Cancer Res* 14: 1266-1273, 2008.
32. Ju X, Liang S, Zhu J, Ke G, Wen H and Wu X: Extracellular matrix metalloproteinase inducer (CD147/BSG/EMMPRIN)-induced radioresistance in cervical cancer by regulating the percentage of the cells in the G2/m phase of the cell cycle and the repair of DNA Double-strand Breaks (DSBs). *Am J Transl Res* 8: 2498-2511, 2016.
33. Zheng H, Wang S, Zhou P, Liu W and Ni F: Effects of Ligustrazine on DNA damage and apoptosis induced by irradiation. *Environ Toxicol Pharmacol* 36: 1197-1206, 2013.
34. Özyurt H, Çevik Ö, Özgen Z, Özden AS, Çadırcı S, Elmas MA, Ercan F, Gören MZ and Şener G: Quercetin protects radiation-induced DNA damage and apoptosis in kidney and bladder tissues of rats. *Free Radic Res* 48: 1247-1255, 2014.
35. Jendrossek V: The intrinsic apoptosis pathways as a target in anticancer therapy. *Curr Pharm Biotechnol* 13: 1426-1438, 2012.
36. Dewey WC, Ling CC and Meyn RE: Radiation-induced apoptosis: Relevance to radiotherapy. *Int J Radiat Oncol Biol Phys* 33: 781-796, 1995.
37. Yang Y, Li XJ, Chen Z, Zhu XX, Wang J, Zhang LB, Qiang L, Ma YJ, Li ZY, Guo QL and You QD: Wogonin induced calreticulin/annexin A1 exposure dictates the immunogenicity of cancer cells in a PERK/AKT dependent manner. *PLoS One* 7: e50811, 2012.
38. Petrella A, Festa M, Ercolino SF, Zerilli M, Stassi G, Solito E and Parente L: Induction of annexin-1 during TRAIL-induced apoptosis in thyroid carcinoma cells. *Cell Death Differ* 12: 1358-1360, 2005.
39. Chang L, Graham PH, Hao J, Ni J, Bucci J, Cozzi PJ, Kearsley JH and Li Y: PI3K/Akt/mTOR pathway inhibitors enhance radiosensitivity in radioresistant prostate cancer cells through inducing apoptosis, reducing autophagy, suppressing NHEJ and HR repair pathways. *Cell Death Dis* 5: e1437, 2014.
40. Tell R, Heiden T, Granath F, Borg AL, Skog S and Lewensohn R: Comparison between radiation-induced cell cycle delay in lymphocytes and radiotherapy response in head and neck cancer. *Br J Cancer* 77: 643-649, 1998.